JASMAC
Conference of the Japan Society of Microgravity Application

OR2-2

浮遊する Fe-Cu 液滴内部における液相分離と熱流動による相形成

Influence of Liquid Phase Separation and Thermofluidic Effects on Phase Formation in Levitated Fe–Cu Droplets

橘髙 里沙[1], 小畠 秀和[2], 清宮 優作[3], 小澤 俊平[3], 杉岡 健一[4], 石川 毅彦[5], 白鳥 英[1]
Risa KITTAKA [1], Hidekazu KOBATAKE [2], Yusaku SEIMIYA [3], Shumpei OZAWA [3], Ken-ichi SUGIOKA [4], Takehiko ISHIKAWA [5], and Suguru SHIRATORI [1]

1 東京都市大学, Department of Mechanical Systems Engineering, Tokyo City University
2 同志社大学, Organization for Research Initiatives & Development, Doshisha University
3 千葉工業大学, Department of Advanced Materials Science and Engineering, Chiba Institute of Technology
4 富山県立大学, Department of Mechanical Systems Engineering, Toyama Prefectural University
5 宇宙航空研究開発機構, Japan Aerospace Exploration Agency

1. Introduction

High-temperature thermal energy storage (TES) systems require suitable phase change materials (PCMs) to function effectively. Immiscible alloys such as Fe-Cu are candidate PCMs for high-temperature applications. However, a comprehensive database of the thermophysical properties for these alloys, which is necessary for the detailed design of TES systems, is still lacking. In response, the Thermal Storage (TS) Project was initiated to obtain accurate thermophysical properties of these alloy materials for application in engineering design 1).

In the TS Project, an Fe-Cu two-phase alloy, which exhibits small volume changes during phase transition, was selected as the experimental sample. The surface tension and viscosity of the molten droplet are calculated by analyzing its oscillatory behavior using the Electrostatic Levitation Furnace (ELF) aboard the International Space Station. In its supercooled state, the Fe-Cu alloy separates into two liquid phases: an Fe-rich phase and a Cu-rich phase. The phase structure within the droplet is expected to change in a complex manner due to the influence of convection. Although the measured surface tension and viscosity are considered to correspond to the phase exposed on the droplet surface, it is difficult to identify the surface phase from experimental results alone. Therefore, numerical simulations that reproduce the ELF experiments are essential to predict the phase state of the molten droplet during property measurements. The TS Project experiments were completed in July 2023 2).

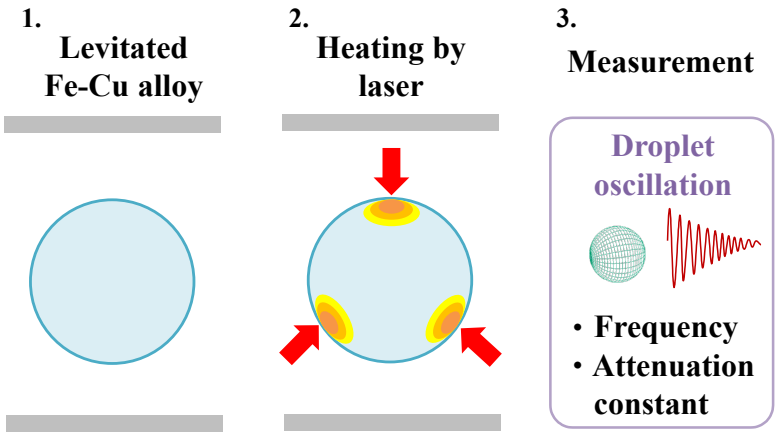

Figure 1. ELF Experiment Overview

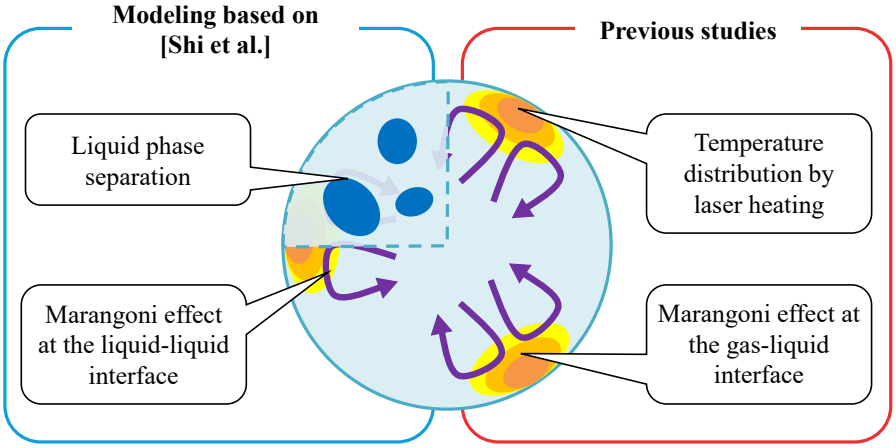

Figure 2. Four elemental models

To accurately simulate the ELF experiments, the physical model must incorporate four key elements:
(1) Temperature distribution by laser heating
(2) Marangoni effect at the gas-liquid interface
(3) Liquid phase separation
(4) Marangoni effect at the liquid-liquid interface
Among these, models for (1) and (2) have already been established in our laboratory through prior research on thermofluidic dynamics in levitated droplets 3). However, models for (3) and (4) were not included. Regarding these phase separation models, Shi et al. have reported a model and simulation examples for the Fe-Cu alloy 4).

However, the work of Shi et al. assumes a gas atomization process for nanoparticle production, and thus their scale and heat transfer models differ significantly from this study. For instance, their model assumes a unidirectional temperature distribution, whereas the ELF employs four-directional laser heating. Furthermore, the droplet scale in their study is 70 nm 200 nm in diameter, compared to the 2 mm diameter sample used in the TS Project. Consequently, a comprehensive model that simultaneously considers all four required elements for the TS Project has not been previously developed. The objective of this research is to build upon prior studies to establish a simulation methodology that integrates these four elements, enabling the discussion of liquid phase separation and thermofluidic effects in levitated Fe-Cu droplets under TS Project experimental conditions.

2. Physical Model and Governing Equations

In this study, a comprehensive model was developed based on the work of Shi et al. 4), incorporating the Marangoni effect at the gas-liquid interface and heat input from lasers. The simulation targets the state inside the droplet after melting and before solidification; the phase change of melting/solidification itself is not considered. Liquid phase separation is calculated using the Cahn-Hilliard equation based on the phase-field method, and this is solved as a coupled system with the flow and temperature fields. The governing equations used in this research are presented below.

$$\nabla \cdot \boldsymbol{u} = 0 \tag{1}$$

$$\rho\left(\frac{\partial \boldsymbol{u}}{\partial t} + \boldsymbol{u}\cdot\nabla\boldsymbol{u}\right) = \nabla\cdot\left(\mu(\nabla\boldsymbol{u} + (\nabla\boldsymbol{u})^{\top})\right) + \nabla\cdot\boldsymbol{\Theta} + \rho\boldsymbol{g} \tag{2}$$

$$\frac{\partial T}{\partial t} + \nabla\cdot(\boldsymbol{u}T) = \nabla\cdot(\alpha\nabla T) \tag{3}$$

$$\frac{\partial c}{\partial t} + \nabla\cdot(\boldsymbol{u}c) = \nabla\cdot\left(M_c\nabla\left(\frac{1}{V_m}\frac{\partial G_m^{\mathrm{liq}}}{\partial c} - \gamma\nabla^2 c\right)\right) + \zeta_c \tag{4}$$

The interfacial stress tensor, $\boldsymbol{\Theta}$, and the bulk Gibbs free energy, G_m^{liq}, are defined as:

$$\boldsymbol{\Theta} = \left[-p + \frac{\gamma}{2}|\nabla c|^2\right]\boldsymbol{I} - \gamma(\nabla c \otimes \nabla c) \tag{5}$$

$$\frac{\partial G_m^{\mathrm{liq}}}{\partial c}(c,T) = G_{\mathrm{Fe}}^{\mathrm{liq}}(T) - G_{\mathrm{Cu}}^{\mathrm{liq}}(T) + RT\ln\left(\frac{c}{1-c}\right) \tag{6}$$

The variables and parameters used in these equations are summarized in Table 1.

Table 1. Nomenclature.

Symbol	Description	Unit
Fluid Dynamics		
$\boldsymbol{u}$	Velocity vector	$\mathrm{m\,s^{-1}}$
ρ	Density	$\mathrm{kg\,m^{-3}}$
μ	Dynamic viscosity	Pa s
p	Pressure	Pa
$\boldsymbol{g}$	Gravitational acceleration	$\mathrm{m\,s^{-2}}$
$\boldsymbol{\Theta}$	Interfacial stress tensor	Pa
Phase Separation and Thermodynamics		
c	Concentration of Cu (mole fraction)	-
T	Temperature	K
α	Thermal diffusivity	$\mathrm{m^2\,s^{-1}}$
V_m	Molar volume of liquid	$\mathrm{m\,mol^{-3}}$
M_c	Atomic mobility	$\mathrm{m^5/Js}$
γ	Interfacial tension coefficient	$\mathrm{J\,m^{-1}}$
ζ_c	Thermal fluctuation term	$\mathrm{s^{-1}}$
R	Universal gas constant	$\mathrm{J\,mol^{-1}\,K^{-1}}$
$\boldsymbol{I}$	Identity tensor	-

3. Methodology

3.1. Numerical Implementation

The coupled system of equations was implemented within the open-source CFD framework OpenFOAM by extending a transient, incompressible solver. This implementation utilizes the PIMPLE algorithm for pressure-velocity coupling, providing a robust method for transient simulations. Custom boundary conditions were developed to accurately represent the experimental setup. A specialized boundary condition is used to model the thermal balance at the droplet surface, which dynamically calculates the surface temperature by accounting for convective cooling, radiative cooling, and the spatially distributed heat flux from the lasers. Furthermore, another boundary condition is applied to the velocity field to model the thermocapillary flow (Marangoni effect) by imposing a shear stress on the free surface proportional to the local surface temperature gradient.

3.2. Material Parameters and Simulation Settings

Fluid properties used in the simulation, such as density ρ and dynamic viscosity μ, are based on thermophysical data for Fe-Cu alloys. On the other hand, parameters specific to the phase separation model, such as the interfacial tension coefficient γ and atomic mobility M_c, must be set based on physical models and literature values. A key challenge in this simulation is the numerical instability arising from the multiscale nature of the problem, where a physically realistic, nanometer-scale interface must be modeled within a millimeter-scale droplet domain. Addressing this instability is a primary focus of the current study. Simulations are performed in a 2D axisymmetric domain representing a 2 mm diameter droplet. The mesh is structured with a higher resolution in the radial direction to capture surface and internal phenomena. The initial composition is set to uniform with small, superimposed random perturbations to trigger the spinodal decomposition process. The microgravity environment of the ELF is modeled by setting the gravitational acceleration vector to $\mathbf{g} = \mathbf{0}$. A small, constant time step is used to ensure numerical stability, particularly during the rapid initial stages of phase separation.

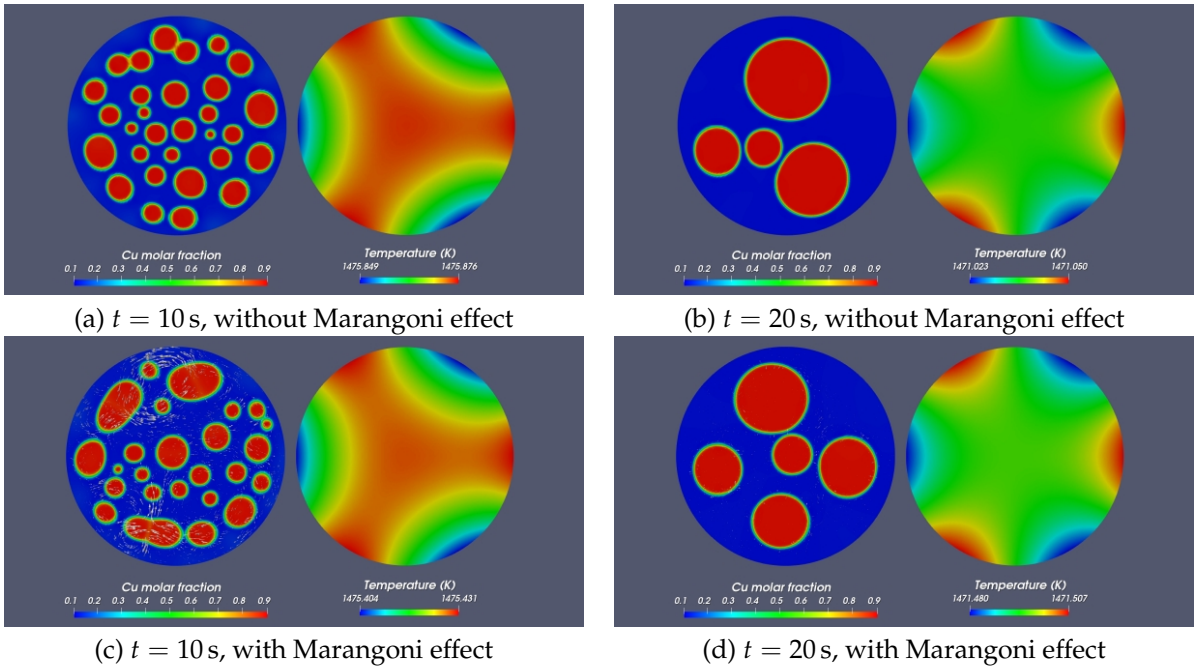

(a) $t = 10\,\mathrm{s}$, without Marangoni effect

(b) $t = 20\,\mathrm{s}$, without Marangoni effect

(c) $t = 10\,\mathrm{s}$, with Marangoni effect

(d) $t = 20\,\mathrm{s}$, with Marangoni effect

Figure 3. Selected snapshots of Cu mole fraction (left) and temperature (right) distribution. (a,b) The case of no Marangoni effect. (c,d) The case where the Marangoni effect is considered.

4. Results

Figure 3 shows some selected snapshots of the mole fraction of Cu C and temperature distribution. For comparison, two different cases were executed; one is the case without the Marangoni effect, and for the other, the Marangoni effect is taken into account. The initial mole fraction is $C = 0.4$ for both cases. To model the ELF experiment, the laser heating and radiation are considered in the heat boundary condition at the free surface. Since we are interested in the time range when the surface tension and viscosity are measured, the laser input is very small, so the intensity of the Marangoni effect is not strong. In **Fig. 3**(a,b), where the Marangoni effect is not taken into account, it can be seen that the spinodal decompositions are clearly expressed in the present model. At the early time state, many small Cu droplets are generated, then they are merged as time progresses. Even when the Marangoni effect is considered, as shown in **Fig. 3**(c,d), the behavior of spinodal decomposition is qualitatively similar to the case of no Marangoni effect. Only small difference can be seen in **Fig. 3**(c), where the merging of the droplets started earlier than that in **Fig. 3**(a). At the conference, we will show more cases and detailed discussions.

References

1) Japan Aerospace Exploration Agency. Thermal Storage Project. Available online: https://humans-in-space.jaxa.jp/kibouser/subject/science/73004.html (accessed on 14 August 2025).
2) Japan Aerospace Exploration Agency. TS Project Experiment Completion. Available online: https://humans-in-space.jaxa.jp/kibouser/pickout/73675.html (accessed on 14 August 2025).
3) Usui, T.; et al. *Int. J. Microgravity Sci. Appl.* **2023**, *40*, 400302.
4) Shi, R.P.; et al. *Acta Mat.* **2013**, *61*, 1229.